

Signature of Mobile Hydrogen Bonding of Lysine Side Chains from Long-Range ^{15}N – ^{13}C Scalar J -Couplings and ComputationLevani Zandarashvili,[†] Da-Wei Li,[†] Tianzhi Wang,[†] Rafael Brüschweiler,[†] and Junji Iwahara^{*,†}[†]Department of Biochemistry and Molecular Biology, Sealy Center for Structural Biology and Molecular Biophysics, University of Texas Medical Branch, Galveston, Texas 77555, United States^{*}Chemical Sciences Laboratory, Department of Chemistry & Biochemistry, and National High Magnetic Field Laboratory, Florida State University, Tallahassee, Florida 32306, United States

S Supporting Information

ABSTRACT: Amino acid side chains involved in hydrogen bonds and electrostatic interactions are crucial for protein function. However, detailed investigations of such side chains in solution are rare. Here, through the combination of long-range ^{15}N – ^{13}C scalar J -coupling measurements and an atomic-detail molecular dynamics (MD) simulation, direct insight into the structural dynamic behavior of lysine side chains in human ubiquitin has been gained. On the basis of $^1\text{H}/^{13}\text{C}/^{15}\text{N}$ heteronuclear correlation experiments selective for lysine NH_3^+ groups, we analyzed two different types of long-range ^{15}N – ^{13}C J -coupling constants: one between intrareidue $^{15}\text{N}\zeta$ and $^{13}\text{C}\gamma$ nuclei ($^3J_{\text{N}\zeta\text{C}\gamma}$) and the other between $^{15}\text{N}\zeta$ and carbonyl $^{13}\text{C}'$ nuclei across a hydrogen bond ($^3J_{\text{N}\zeta\text{C}'}$). The experimental $^3J_{\text{N}\zeta\text{C}\gamma}$ data confirm the highly mobile nature of the χ_4 torsion angles of lysine side chains seen in the MD simulation. The NH_3^+ groups of Lys29 and Lys33 exhibit measurable $^3J_{\text{N}\zeta\text{C}'}$ couplings arising from hydrogen bonds with backbone carbonyl groups of Glu16 and Thr14, respectively. When interpreted together with the $^3J_{\text{N}\zeta\text{C}\gamma}$ -coupling constants and NMR-relaxation-derived S^2 order parameters of the NH_3^+ groups, they strongly suggest that hydrogen bonds involving NH_3^+ groups are of a transient and highly dynamic nature, in remarkably good agreement with the MD simulation results.

Protein side chains play vital roles in molecular function, such as enzymatic catalysis and protein–protein interactions. Although structural biology has provided important insights into the side-chain behavior of proteins and their complexes, the functional role of side-chain dynamics is not well understood. Powerful NMR techniques for the investigation of protein dynamics exist, but the vast majority are applicable only to the backbone or methyl groups.¹ The lack of specific experiments for characterizing the dynamics of side chains involved in hydrogen bonds and electrostatic interactions therefore represents a bottleneck in understanding structure–dynamics–function relationships in proteins.

We recently developed new NMR methods to characterize lysine side-chain amino groups,^{2–5} including the design of ^{15}N relaxation experiments for the extraction of side-chain S^2 order parameters.⁵ For ubiquitin, the majority of the lysine NH_3^+ groups display notably low S^2 order parameters, reflecting a high degree of internal mobility for these functionally important

entities, with correlation times in the subnanosecond range for the NH_3^+ bond rotations. However, the origin of the side-chain mobility could not be elucidated from experiment alone. On the basis of intra- and interresidual long-range ^{15}N – ^{13}C scalar J -coupling constants, we have found in the present work that the mobility about the χ_4 torsion angle of lysine side chains is generally high. Hydrogen bonds formed by the NH_3^+ groups therefore have a highly transient character. The experimental results have been quantitatively compared with an extended molecular dynamics (MD) simulation.

We report here two different types of long-range ^{15}N – ^{13}C J -coupling constants involving the lysine NH_3^+ groups: the intrareidue J -coupling between $^{15}\text{N}\zeta$ and $^{13}\text{C}\gamma$ nuclei ($^3J_{\text{N}\zeta\text{C}\gamma}$) and the J -coupling between $^{15}\text{N}\zeta$ and carbonyl $^{13}\text{C}'$ nuclei across a $\text{N}\zeta\text{--H}\zeta\cdots\text{O}=\text{C}'$ hydrogen bond ($^3J_{\text{N}\zeta\text{C}'}$). Figure 1 shows the lysine-specific NMR pulse sequences for measuring the absolute values of the J -coupling constants between the $^{15}\text{N}\zeta$ and ^{13}C nuclei. Because of the unique ^{15}N chemical shifts of NH_3^+ groups (~ 33 ppm), these pulse sequences permit selective observation of lysine NH_3^+ groups in a uniformly $^{13}\text{C}/^{15}\text{N}$ -labeled protein. The remarkably slow relaxation of the in-phase single-quantum N_+ terms for NH_3^+ groups^{2,5} permits the use of relatively long periods for the evolution of ^{15}N transverse magnetizations in order to measure the small ^{15}N – ^{13}C J -coupling constants. Using these pulse sequences, we recorded the data for 1 mM $^{13}\text{C}/^{15}\text{N}$ -labeled ubiquitin at pH 5 and 2 °C. The low pH and temperature were necessary to make the hydrogen exchange sufficiently slow that lysine NH_3^+ protons could be observed.⁵

The pulse sequence in Figure 1A corresponds to a two-dimensional heteronuclear correlation experiment to observe signals arising from coherence transfer via ^{15}N – ^{13}C J -coupling for lysine NH_3^+ groups. The F_2 dimension corresponds to $^1\text{H}\zeta$ chemical shifts of the NH_3^+ groups and the F_1 dimension to ^{13}C chemical shifts of nuclei coupled to $^{15}\text{N}\zeta$. In the spectrum recorded with this pulse sequence, ($^{13}\text{C}\gamma$, $^1\text{H}\zeta$) cross-peaks were clearly observed for all lysine residues, indicating that the χ_4 -related $^3J_{\text{N}\zeta\text{C}\gamma}$ values are sizable (Figure 2A). Although the ^{13}C IBURP-2 pulses covered the lysine $^3\text{C}\gamma/^{13}\text{C}\delta$ region (23–30 ppm), no $^{13}\text{C}\delta$ signals were observed in the spectrum. The absence of the $^{13}\text{C}\delta$ signals suggested that $^2J_{\text{N}\zeta\text{C}\delta} < 0.2$ Hz (as estimated from the noise level). For the quantitative measurement of $^3J_{\text{N}\zeta\text{C}\gamma}$ values, we used the spin-echo $^{15}\text{N}\{^{13}\text{C}\}$

Received: March 10, 2011

Published: May 19, 2011

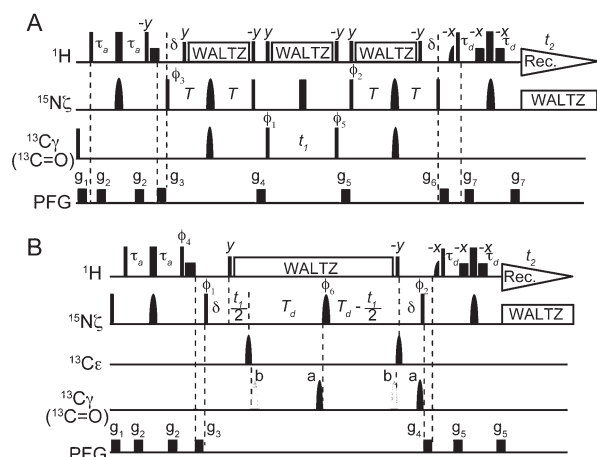


Figure 1. (A) Pulse sequence for observing heteronuclear correlation via long-range ^{15}N – ^{13}C 3J -coupling for lysine side-chain NH_3^+ groups. (B) Constant-time spin-echo difference ^1H – ^{15}N correlation experiment to measure $^3J_{\text{NCCY}}$ and $^3J_{\text{NCC}'}$ for lysine NH_3^+ groups. Thin and bold bars in black represent hard rectangular 90° and 180° pulses, respectively. Unless indicated otherwise, pulse phases are along x . Carrier positions: ^1H , the position of the water resonance; ^{15}N , 33 ppm; $^{13}\text{C}_\gamma$, 23 ppm; $^{13}\text{C}_\epsilon$, 45 ppm; and $^{13}\text{C}=\text{O}$, 177 ppm. In (B), two data sets were recorded in an interleaved manner, with the two ^{13}C IBURP-2 pulses⁶ located at either positions a or b. Pulsed field gradients were optimized to minimize the water signal. Short bold bars represent water-selective soft-rectangular ^1H 90° pulses (1.2 ms). Shaped pulses: ^1H half-Gaussian 90° pulse (2.1 ms); ^{15}N r-SNOB 180° pulse⁷ (1.03 ms); and ^{13}C IBURP-2 180° pulses (1.1 ms). Delays: $\tau_a = 2.7$ ms, $\delta = 2.6$ ms, $T = 50$ ms, and $T_d = 104$ ms for the $^3J_{\text{NCCY}}$ experiments; $T = 106$ ms and $T_d = 212$ ms for the $^3J_{\text{NCC}'}$ experiments. Phase cycles: $\phi_1 = \{2x, 2(-x)\}$, $\phi_2 = \{4x, 4(-x)\}$, $\phi_3 = \{x, -x\}$, $\phi_4 = \{y, -y\}$, $\phi_5 = \{8x, 8(-x)\}$, $\phi_6 = \{8x, 8y, 8(-x), 8(-y)\}$, and receiver = $\{x, -x, -x, x, x, 2(-x, x, x, -x), x, -x, -x, x\}$. Quadrature detection in the t_1 domain was achieved using States-TPPI for ϕ_1 . The experiments were carried out using a Varian NMR system operated at a ^1H frequency of 800 MHz.

difference experiment shown in Figure 1B. In this experiment, which is analogous to those developed for measuring χ_1 -related $^3J_{\text{NCCY}}$ -coupling constants,⁸ two subspectra were recorded in an interleaved manner: one with the $^{13}\text{C}_\gamma$ -selective IBURP-2 pulses at positions a (subspectrum a) and the other at positions b (subspectrum b). The net evolution time for $^3J_{\text{NCCY}}$ -coupling for ^{15}N transverse magnetizations is $2(T_d + \delta)$ for the former case and zero for the latter. The values of $^3J_{\text{NCCY}}$ can be calculated from the expression $I_a/I_b = \cos[2\pi J_{\text{NCCY}}(T_d + \delta)]$, in which I_a and I_b represent the signal intensities in subspectra a and b, respectively. Table 1 shows the values of $^3J_{\text{NCCY}}$ obtained for lysine side chains in ubiquitin. The precision of the measured coupling constants was high because of the very slow ^{15}N relaxation of the NH_3^+ groups, which allowed the use of a long period for J modulation (209 ms).

The $^3J_{\text{NCCY}}$ -coupling constants were subsequently interpreted by means of Karplus equations.¹⁹ Because empirical Karplus parameters are not available for $^3J_{\text{NCCY}}$ reporting on the torsion angle χ_4 , here we used the experimental Karplus parameters for $^3J_{\text{NCY}}$ belonging to χ_1 reported by Pérez et al.¹⁰ On the basis of these parameters, $^3J_{\text{NCCY}}$ values were back-calculated first from the χ_4 angles in the 1.8 Å resolution X-ray crystal structure of ubiquitin (PDB entry 1UBQ).¹¹ As shown in Figure 2B, a bimodal distribution around ~ 2 and ~ 0.5 Hz was found for the calculated values of $^3J_{\text{NCCY}}$ because the lysine χ_4 angles in the crystal structure are either trans or gauche. In contrast, the experimental $^3J_{\text{NCCY}}$ data do not exhibit such a bimodal distribution, and the agreement

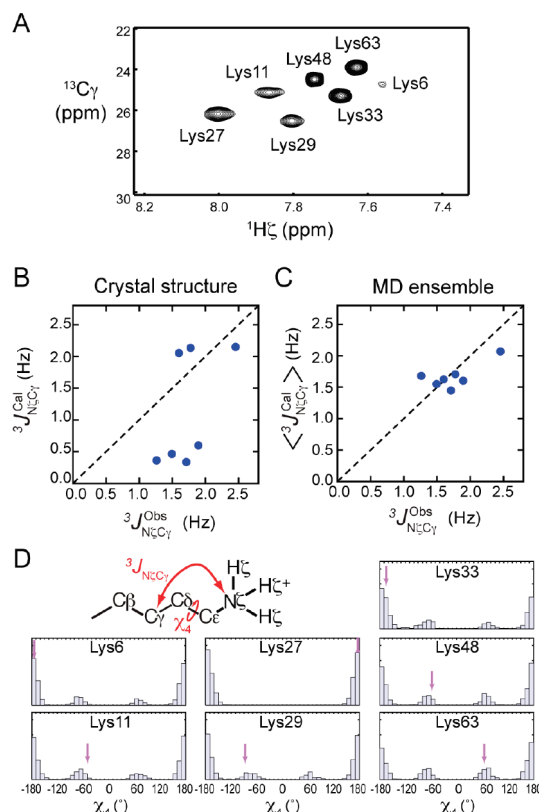


Figure 2. (A) Long-range correlation spectra recorded with the pulse sequence shown in Figure 1A for lysine side-chain NH_3^+ groups in uniformly $^{13}\text{C}/^{15}\text{N}$ -labeled ubiquitin. The ^{13}C IBURP-2 pulses were applied at 23 ppm. (B) Correlation between the observed $^3J_{\text{NCCY}}$ values and those calculated from the crystal structure (PDB entry 1UBQ). (C) Correlation between the observed $^3J_{\text{NCCY}}$ values and those calculated as ensemble averages for 1000 structures sampled every 1 ns from the 1 μs MD trajectory at 275 K. (D) Histograms of the χ_4 torsion angles of individual lysine side chains of the MD ensemble. Purple arrows indicate the χ_4 torsion angles in the crystal structure.

between the observed and calculated $^3J_{\text{NCCY}}$ data was poor, with a root-mean-square difference (rmsd) of 0.91 Hz (Figure 2B).

We also examined the ensemble averages ($\langle ^3J_{\text{NCCY}} \rangle$) calculated from the χ_4 angles sampled during a 1 μs MD simulation at 275 K using the GROMACS software package¹² and the AMBER ff99SB force field.¹³ To ensure a fair comparison, the simulation was run at the same temperature as in the experiment; otherwise, the MD simulation protocol was the same as described previously.⁵ The length of the MD simulation was expected to be adequate for this analysis, since our previous NMR relaxation study showed that the reorientation of the symmetry axes of lysine NH_3^+ groups in ubiquitin occurs on the subnanosecond time scale.⁵ Values of $\langle ^3J_{\text{NCCY}} \rangle$ were calculated from 1000 MD snapshots sampled every 1 ns. As shown in Figure 2C, the $\langle ^3J_{\text{NCCY}} \rangle$ data from the MD ensemble exhibited substantially improved agreement with the experimental $^3J_{\text{NCCY}}$ data (rmsd = 0.26 Hz). As shown in the Supporting Information (SI), direct fitting of the Karplus parameters to the MD ensemble¹⁴ resulted in only a slight reduction of the rmsd (0.25 Hz), and the optimized Karplus parameters and the empirical parameters for χ_1 -related $^3J_{\text{NCCY}}$ -couplings gave almost the same $^3J_{\text{NCCY}}$ values (rmsd = 0.06 Hz). This suggests that the empirical parameters of Pérez et al. represent an adequate choice for the $^3J_{\text{NCCY}}$ -couplings analyzed here. The large difference between the $^3J_{\text{NCCY}}$ values calculated from the crystal structure

Table 1. Long-Range ^{15}N – ^{13}C J -Coupling Constants $^3J_{\text{N}\zeta\text{C}\gamma}$ and $^3J_{\text{N}\zeta\text{C}'}$ Measured for Lysine Side-Chain NH_3^+ Groups in Human Ubiquitin^a

NH_3^+	$^3J_{\text{N}\zeta\text{C}\gamma}$ (Hz) ^b	$^3J_{\text{N}\zeta\text{C}'}$ (Hz) ^c
Lys6	1.78 ± 0.25	—
Lys11	1.89 ± 0.03	—
Lys27	2.45 ± 0.03	—
Lys29	1.26 ± 0.03	0.23 ± 0.03 (Glu16 C=O) ^d
Lys33	1.60 ± 0.01	0.17 ± 0.02 (Thr14 C=O) ^d
Lys48	1.49 ± 0.01	—
Lys63	1.71 ± 0.01	—

^a The J -coupling constants were measured using spin-echo $^{15}\text{N}\{^{13}\text{C}\}$ difference experiments (Figure 1B) at a ^1H frequency of 800 MHz. Only absolute values are reported because the measurements did not provide signs. ^b Measured three times to improve the precision. Averages and standard deviations are shown. ^c Measured once. Uncertainties were estimated from the noise levels in the spectra. ^d The acceptor of the hydrogen bond, which was identified in the long-range correlation spectrum (Figure 3A), is shown in parentheses.

and the $\langle ^3J_{\text{N}\zeta\text{C}\gamma} \rangle$ values obtained from the MD ensemble is due to the wide distribution of χ_4 angles observed in the MD ensemble, which reflects extensive rotameric interconversions of this torsion angle (Figure 2D). Hence, the agreement between the experimental $^3J_{\text{N}\zeta\text{C}\gamma}$ data and those predicted from the MD trajectory strongly indicates that the lysine χ_4 dihedral angles in ubiquitin are highly dynamic. This result is consistent with the low values of the order parameters found for most of the lysine C_ϵ – $\text{N}_\zeta\text{H}_3^+$ vectors in our recent ^{15}N relaxation study.⁵

While it has been well-established that internal motions changing the bond torsion angles directly affect the relevant vicinal 3J -coupling constants, the derivation of quantitative dynamics information from 3J -coupling data is not straightforward.^{10,15} By far the easiest interpretation of 3J -coupling data entails the extraction of structural information on relatively static portions of molecules.¹ As demonstrated above, the combined use of a long MD simulation and 3J -coupling data permits a direct consistency analysis of the torsion-angle dynamics of protein side chains. Using our previous trajectory from a 1 μs MD simulation at 300 K,⁵ we also examined the impact of the dynamics on the χ_1 -related $^3J_{\text{N}\zeta\text{C}\gamma}$ -coupling constants (through $\text{N}-\text{C}\alpha-\text{C}\beta-\text{C}\gamma$) for ubiquitin using the experimental data at 303 K reported by Hu and Bax.^{8b} As shown in the SI, the experimental $^3J_{\text{N}\zeta\text{C}\gamma}$ data for arginine, lysine, glutamate, and glutamine residues exhibited far better correlation with those calculated from the MD ensemble than with those calculated from the crystal structure. This suggests that the χ_1 torsion angles of these solvent-exposed hydrophilic side chains are highly dynamic, as seen in the MD simulation. It should be noted that the $\langle ^3J \rangle$ values from the MD ensemble depend on the molecular mechanics force field used for the simulation. Hence, the degree of the agreement between the $\langle ^3J \rangle$ values from the MD simulation and the experimental 3J -coupling constants is expected to be directly useful for benchmarking and improving future MD force fields using NMR data for full-length proteins in their native environments.¹⁶

In order to gain direct insight into hydrogen bonds involving the lysine side chains, we also studied ^{15}N – ^{13}C 3J -coupling constants $^3J_{\text{N}\zeta\text{C}'}$ across hydrogen bonds involving lysine NH_3^+ groups of ubiquitin. Figure 3A shows the long-range correlation spectrum recorded for lysine NH_3^+ groups. Because of $^{13}\text{C}=\text{O}$ -selective IBURP-2 pulses that do not affect aliphatic ^{13}C nuclei, only NH_3^+ groups having sizable J -couplings with carbonyl or

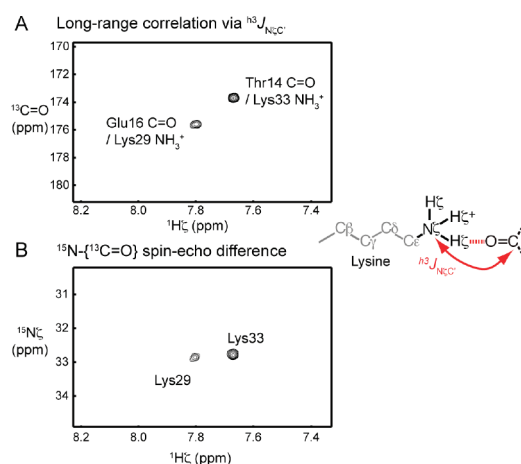


Figure 3. (A) Long-range correlations via $^3J_{\text{N}\zeta\text{C}'}$ -coupling across $\text{NH}_3^+ \cdots \text{O}=\text{C}$ hydrogen bonds. This spectrum was recorded using the pulse sequence shown in Figure 1A. (B) Spin-echo $^{15}\text{N}\{^{13}\text{C}=\text{O}\}$ difference spectrum for the two subspectra recorded with $^{13}\text{C}=\text{O}$ -selective pulses at positions a and b in the pulse sequence shown in Figure 1B.

carboxyl ^{13}C nuclei across a hydrogen bond can give signals in this experiment. Signals for Lys29 and Lys33 NH_3^+ groups were clearly observed in the long-range correlation spectrum. The ^{13}C chemical shifts for the signals observed for the Lys29 and Lys33 NH_3^+ groups are in excellent agreement with those of backbone $\text{C}=\text{O}$ groups of Glu16 and Thr14, respectively. In fact, these carbonyl groups are in close proximity to the lysine NH_3^+ groups in the crystal structure: the distances between the donor N_ζ and acceptor O atoms are 2.7 Å for the Lys29–Glu16 pair and 3.5 Å for the Lys33–Thr14 pair. In the 1 μs MD simulation, the overall occupancies of the hydrogen bonds (N_ζ – O distance < 3.5 Å) were 80% for the Lys29–Glu16 pair and 51% for the Lys33–Thr14 pair. The existence of the NMR signals arising from $^3J_{\text{N}\zeta\text{C}'}$ -coupling provides direct evidence for at least a part-time presence of these hydrogen bonds in solution.

To determine the values of $^3J_{\text{N}\zeta\text{C}'}$, we carried out the spin-echo $^{15}\text{N}\{^{13}\text{C}=\text{O}\}$ difference constant-time ^1H – ^{15}N correlation experiment for the lysine NH_3^+ groups, as shown in Figure 1B. The difference spectrum for the two subspectra a and b gives signals only if intensity modulation by $^3J_{\text{N}\zeta\text{C}'}$ evolution is sizable. As expected from the result of the long-range correlation experiment, only the NH_3^+ groups of Lys29 and Lys33 exhibited signals in the difference spectrum (Figure 3B). The values of $^3J_{\text{N}\zeta\text{C}'}$ were determined to be 0.23 and 0.17 Hz for the Lys29–Glu16 and Lys33–Thr14 hydrogen bonds, respectively (Table 1). These values are relatively small in comparison with the $^3J_{\text{N}\zeta\text{C}'}$ values for hydrogen bonds between backbone $\text{N}-\text{H}$ and $\text{C}=\text{O}$ groups, which can reach 0.9 Hz.¹⁷ Since a scalar coupling across a hydrogen bond depends on the electronic configuration, the average geometry,¹⁸ and internal motions,¹⁹ quantitative interpretation of the observed $^3J_{\text{N}\zeta\text{C}'}$ values for the NH_3^+ groups is not possible at this point. Nonetheless, the observed $^3J_{\text{N}\zeta\text{C}'}$ -couplings unequivocally indicate the part-time presence of hydrogen bonds between the NH_3^+ and $\text{C}=\text{O}$ groups. Dynamic hydrogen bonding displayed by lysine side-chain NH_3^+ groups arises from the highly mobile χ_4 torsion angles combined with rapid rotation about the C_3 symmetry axis along the N_ζ – C_ϵ bond, as depicted in Figure 4 for Lys29 and Lys33. In our previous ^{15}N relaxation study,⁵ the order parameters for the NH_3^+ groups of the same amino acids indicated high mobility on the subnanosecond time scale ($S_{\text{axis}}^2 = 0.38$ for Lys29 and 0.25 for Lys33).

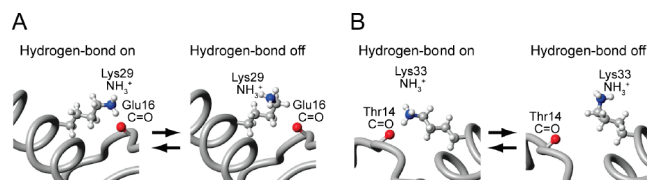


Figure 4. Dynamics of (A) Lys29–Glu16 and (B) Lys33–Thr14 hydrogen bonds seen in a 1 μ s MD simulation at 275 K. The acceptors are backbone carbonyl groups. These hydrogen bonds were experimentally confirmed by means of measured $^3J_{\text{N}\alpha\text{C}\gamma}$ values (Figure 3). The average lifetimes of the hydrogen bonds in the MD simulation were 45 and 30 ps for Lys29 and Lys33, respectively.

As shown in Figure 4, the MD simulation also showed a highly dynamic hydrogen-bonding process involving the side-chain NH_3^+ groups of Lys29 and Lys33. Together with the detected $^3J_{\text{N}\alpha\text{C}\gamma}$ -couplings for Lys29 and Lys33, these data collectively suggest that the side-chain hydrogen bonds evidenced by detectable $^3J_{\text{N}\alpha\text{C}\gamma}$ -couplings are of a highly mobile nature.

In conclusion, we have demonstrated the use of long-range ^{15}N – ^{13}C 3J -coupling data for investigating the detailed dynamic behavior of lysine side chains in a protein. In conjunction with an extended MD simulation, the 3J -coupling data provide insights into the side-chain dynamics with regard to hydrogen bonding and torsion angle rotations in a way that is highly complementary to spin-relaxation-based dynamics studies. Taken together, this information will be useful for understanding the relationship between the function and dynamics of hydrogen bonding of lysine side chains, which plays important roles in protein stability,²⁰ biomolecular interactions,²¹ and enzymatic active sites.²² The approach used here can be adapted for studying the structural dynamics of other types of side-chain groups taking part in hydrogen-bond formation and electrostatic interactions (e.g., guanidino groups of arginine).

■ ASSOCIATED CONTENT

S Supporting Information. Effect of internal motions on $^3J_{\text{N}\alpha\text{C}\gamma}$ -coupling constants reporting on side-chain χ_1 torsion angles between backbone ^{15}N and side-chain $^{13}\text{C}\gamma$ nuclei of arginine, glutamine, glutamate, and lysine residues in ubiquitin and direct fitting of Karplus parameters to the MD ensemble. This material is available free of charge via the Internet at <http://pubs.acs.org>.

■ AUTHOR INFORMATION

Corresponding Author

j.iwahara@utmb.edu

■ ACKNOWLEDGMENT

This work was supported by Grants MCB-0918362 (to R.B.) and MCB-0920238 (to J.I.) from the National Science Foundation, Grant 49968-DNI4 from the American Chemical Society Petroleum Research Fund (to J.I.), and Grant H-1683 from the Welch Foundation (to J.I.).

■ REFERENCES

- (1) Cavanagh, J.; Fairbrother, W. J.; Palmer, A. G., III; Rance, M.; Skelton, N. J. *Protein NMR Spectroscopy: Principles and Practice*, 2nd ed.; Elsevier Academic Press: Burlington, MA, 2007.
- (2) Iwahara, J.; Jung, Y. S.; Clore, G. M. *J. Am. Chem. Soc.* **2007**, *129*, 2971.
- (3) Takayama, Y.; Castañeda, C. A.; Chimenti, M.; García-Moreno, B.; Iwahara, J. *J. Am. Chem. Soc.* **2008**, *130*, 6714.

- (4) Takayama, Y.; Sahu, D.; Iwahara, J. *J. Magn. Reson.* **2008**, *194*, 313.
- (5) Esadze, A.; Li, D. W.; Wang, T.; Brüschweiler, R.; Iwahara, J. *J. Am. Chem. Soc.* **2011**, *133*, 909.
- (6) Geen, H.; Freeman, R. J. *Magn. Reson.* **1991**, *93*, 93.
- (7) Kupče, E.; Boyd, J.; Campbell, I. D. J. *Magn. Reson., Ser. B* **1995**, *106*, 300.
- (8) (a) Bax, A.; Vuister, G. W.; Grzesiek, S.; Delaglio, F.; Wang, A. C.; Tschudin, R.; Zhu, G. *Methods Enzymol.* **1994**, *239*, 79. (b) Hu, J. S.; Bax, A. *J. Biomol. NMR* **1997**, *9*, 323. (c) Hu, J. S.; Grzesiek, S.; Bax, A. *J. Am. Chem. Soc.* **1997**, *119*, 1803.
- (9) Karplus, M. *J. Chem. Phys.* **1959**, *30*, 11.
- (10) Pérez, C.; Löhr, F.; Rüterjans, H.; Schmidt, J. M. *J. Am. Chem. Soc.* **2001**, *123*, 7081.
- (11) Vijay-Kumar, S.; Bugg, C. E.; Cook, W. J. *J. Mol. Biol.* **1987**, *194*, 531.
- (12) van der Spoel, D.; Lindahl, E.; Hess, B.; Groenhof, G.; Mark, A. E.; Berendsen, H. J. C. *J. Comput. Chem.* **2005**, *26*, 1701.
- (13) Hornak, V.; Abel, R.; Okur, A.; Strockbine, B.; Roitberg, A.; Simmerling, C. *Proteins* **2006**, *65*, 712.
- (14) Markwick, P. R. L.; Showalter, S. A.; Bouvignies, G.; Brüschweiler, R.; Blackledge, M. *J. Biomol. NMR* **2009**, *45*, 17.
- (15) (a) Pachler, K. G. R. *Spectrochim. Acta* **1963**, *19*, 2085. (b) Pachler, K. G. R. *Spectrochim. Acta* **1964**, *20*, 581. (c) Gibbons, W. A.; Nemethy, G.; Stern, A.; Craig, L. C. *Proc. Natl. Acad. Sci. U.S.A.* **1970**, *67*, 239. (d) Rinkel, L. J.; Altona, C. J. *Biomol. Struct. Dyn.* **1987**, *4*, 621. (e) Madi, Z. L.; Griesinger, C.; Ernst, R. R. *J. Am. Chem. Soc.* **1990**, *112*, 2908. (f) Dzakula, Z.; Edison, A. S.; Westler, W. M.; Markley, J. L. *J. Am. Chem. Soc.* **1992**, *114*, 6200. (g) Dzakula, Z.; Westler, W. M.; Edison, A. S.; Markley, J. L. *J. Am. Chem. Soc.* **1992**, *114*, 6195. (h) van Wijk, J.; Huckriede, B. D.; Ippel, J. H.; Altona, C. *Methods Enzymol.* **1992**, *211*, 286. (i) Brunne, R. M.; van Gunsteren, W. F.; Brüschweiler, R.; Ernst, R. R. *J. Am. Chem. Soc.* **1993**, *115*, 4764. (j) Schmidt, J. M.; Brüschweiler, R.; Ernst, R. R.; Dunbrack, R. L.; Joseph, D.; Karplus, M. *J. Am. Chem. Soc.* **1993**, *115*, 8747. (k) Brüschweiler, R.; Case, D. A. *J. Am. Chem. Soc.* **1994**, *116*, 11199. (l) Case, D. A.; Scheurer, C.; Brüschweiler, R. *J. Am. Chem. Soc.* **2000**, *122*, 10390. (m) Chou, J. J.; Case, D. A.; Bax, A. *J. Am. Chem. Soc.* **2003**, *125*, 8959.
- (16) (a) Best, R. B.; Hummer, G. *J. Phys. Chem. B* **2009**, *113*, 9004. (b) Wickstrom, L.; Okur, A.; Simmerling, C. *Biophys. J.* **2009**, *97*, 853. (c) Lindorff-Larsen, K.; Piana, S.; Palmo, K.; Maragakis, P.; Klepeis, J. L.; Dror, R. O.; Shaw, D. E. *Proteins* **2010**, *78*, 1950. (d) Li, D. W.; Brüschweiler, R. *Angew. Chem., Int. Ed.* **2010**, *49*, 6778. (e) Li, D.-W.; Brüschweiler, R. *J. Chem. Theory Comput.* [Online early access]. DOI: 10.1021/ct200094b. Published Online: May 5, 2011.
- (17) (a) Cordier, F.; Grzesiek, S. *J. Am. Chem. Soc.* **1999**, *121*, 1601. (b) Cornilescu, G.; Hu, J. S.; Bax, A. *J. Am. Chem. Soc.* **1999**, *121*, 2949. (c) Cornilescu, G.; Ramirez, B. E.; Frank, M. K.; Clore, G. M.; Gronenborn, A. M.; Bax, A. *J. Am. Chem. Soc.* **1999**, *121*, 6275. (d) Wang, Y. X.; Jacob, J.; Cordier, F.; Wingfield, P.; Stahl, S. J.; Lee-Huang, S.; Torchia, D.; Grzesiek, S.; Bax, A. *J. Biomol. NMR* **1999**, *14*, 181. (e) Grzesiek, S.; Cordier, F.; Jaravine, V.; Barfield, M. *Prog. NMR Spectrosc.* **2004**, *45*, 275.
- (18) (a) Scheurer, C.; Brüschweiler, R. *J. Am. Chem. Soc.* **1999**, *121*, 8661. (b) Czernek, J.; Brüschweiler, R. *J. Am. Chem. Soc.* **2001**, *123*, 11079. (c) Barfield, M. *J. Am. Chem. Soc.* **2002**, *124*, 4158.
- (19) (a) Bouvignies, G.; Bernado, P.; Meier, S.; Cho, K.; Grzesiek, S.; Brüschweiler, R.; Blackledge, M. *Proc. Natl. Acad. Sci. U.S.A.* **2005**, *102*, 13885. (b) Juranic, N.; Atanasova, E.; Streiff, J. H.; Macura, S.; Prendergast, F. G. *Protein Sci.* **2007**, *16*, 1329. (c) Saas, H. J.; Schmid, F. F.; Grzesiek, S. *J. Am. Chem. Soc.* **2007**, *129*, 5898.
- (20) (a) Marqusee, S.; Baldwin, R. L. *Proc. Natl. Acad. Sci. U.S.A.* **1987**, *84*, 8898. (b) Scholtz, J. M.; Qian, H.; Robbins, V. H.; Baldwin, R. L. *Biochemistry* **1993**, *32*, 9668. (c) Pace, C. N.; Grimsley, G. R.; Scholtz, J. M. *J. Biol. Chem.* **2009**, *284*, 13285.
- (21) (a) Jones, S.; Marin, A.; Thornton, J. M. *Protein Eng.* **2000**, *13*, 77. (b) Luscombe, N. M.; Laskowski, R. A.; Thornton, J. M. *Nucleic Acids Res.* **2001**, *29*, 2860.
- (22) (a) Bartlett, G. J.; Porter, C. T.; Borkakoti, N.; Thornton, J. M. *J. Mol. Biol.* **2002**, *324*, 105. (b) Holliday, G. L.; Mitchell, J. B. O.; Thornton, J. M. *J. Mol. Biol.* **2009**, *390*, 560.